ISSN 2075-3810 (Print), ISSN 2075-3829 (Online)

БІОФІЗИЧНИЙ ВІСНИК, 2024, Вип. 51 BIOPHYSICAL BULLETIN, 2024, Iss. 51

BIOMEDICAL ENGINEERING

Original article
https://doi.org/10.26565/2075-3810-2024-51-02

UDC 616-72+616.8-089

DETERMINING THE RELATIONSHIP BETWEEN THE SPEED OF MOTION OF LARGE PERMANENT MAGNETS AND THE TRAJECTORY OF IMPLANTS IN MAGNETIC STEREOTAXIC SYSTEMS

J. Hankun, O. G. Avrunin
Kharkiv National University of Radio Electronics, 14 Nauky Ave., Kharkiv, 61166, Ukraine
e-mail: 1350829683@qq.com, oleh.avrunin@nure.ua
Submitted November 9, 2023; Revised January 17, 2024;
Accepted March 20, 2024

Background: The magnetic stereotaxic system is a new type of neurosurgical intervention that is in the experimental stage. This method allows the implant to be controlled non-contact by an external magnetic field, allowing it to move along an arbitrary trajectory to a lesion located in a deep structure of the brain tissue to deliver hyperthermia to the lesion site or deliver medication through a catheter. In previous studies, we have found that it is completely feasible for the implant to move along the arc trajectory, so we need to determine the relationship between the movement speed of the large permanent magnet that constitutes the external magnetic field and the implant movement trajectory, so as to control the implant movement more precisely.
Objectives: Investigate the effect of the speed of motion of large permanent magnets, which constitute the external magnetic field, on the trajectory of implants (small permanent magnets).
Materials and Methods: Firstly, three sets of computer simulation experiments were conducted, each group of experiments only changed the operating speed of large permanent magnets, and the changes in the trajectories of small and medium-sized permanent magnets in the three sets of experiments were observed and compared. After that practical experiments are carried out to validate the results of the computer simulation experiments by means of the slide rail system controlled by an Arduino microcontroller.
Results: The relationship between the moving speed of the large permanent magnet and the trajectory of the small permanent magnet was determined by simulation experiments, and the changes in the strength of the surrounding magnetic field during the movement of the implant were calculated. Afterwards, it was verified by practical experiments. The faster the large permanent magnet moves, the shorter the distance that the small permanent magnet moves along the linear trajectory, and the longer the distance that moves along the arc trajectory; The slower the large permanent magnet moves, the longer the small permanent magnet travels along a straight trajectory and the shorter the distance it travels along an arc trajectory.
Conclusions: In this research, we have determined the relationship between the running speed of the large permanent magnet that constitutes the external magnetic field and the implant's moving trajectory by combining computer simulation experiments with practical experiments, i.e., the faster the large permanent magnet moves, the shorter the implant's moving distance is along a straight line trajectory, and the longer the moving distance is along a curved line trajectory. This means that we can control the distance and steering angle of the implant more accurately, which makes the study of the magnetic stereotaxic system further, and lays a theoretical foundation and provides a large amount of experimental data for the implant to be able to reach the diseased site located in the deep structure of the brain tissue along complex pathways in neurosurgical interventions with the participation of the magnetic stereotaxic system.

In cites: Hankun J, Avrunin OG. Determining the relationship between the speed of motion of large permanent magnets and the trajectory of implants in magnetic stereotaxic systems. Biophysical Bulletin. 2024;51:26–38. https://doi.org/10.26565/2075-3810-2024-51-02

KEY WORDS: human health; magnetic field; COMSOL software; permanent magnets; force analysis; Arduino; microcontrollers.

Magnetic stereotaxic system [1–3] is a new experimental high-precision neurosurgical method. In traditional high-precision neurosurgery, stereotaxic devices [4–6] are often used to guide directly surgical intervention by mechanically controlled surgical instruments. However, due to the fact that mechanically controlled surgical instruments can only move along a straight trajectory, the surgical access is limited, which is more harmful to the surrounding tissues on the movement path of the surgical instruments, and it is difficult to reach the deep structure of the brain tissue. As a result, it is difficult to effectively treat brainstem tumors and many extrapyramidal nervous system disorders.

In contrast to traditional surgical methods, the magnetic stereotaxis system consists of a computer-controlled, variable external magnetic field and an implant connected by a catheter. The idea of this method is to first probe the catheter-connected micro-magnetic implant into the brain tissue, and then control the external magnetic field changes through the computer, and guide the implant to move to the lesion located in the deep structure of the brain tissue along the pre-calculated trajectory, so as to provide hyperthermia to the lesion site or deliver drugs through the catheter.

The advantage of this method is that the patient's brain tissue can be scanned by CT and MRI to build an accurate model [7, 8], non-contact control allows the implant to reach almost any position in the brain along any trajectory, less harmful to the surrounding tissues on the path. Therefore, the magnetic stereotaxic system is one of the most promising methods for neurosurgical intervention of brain tissue under current conditions, and at the same time one of the least invasive.

The purpose of this research was to investigate the effect of the speed of motion of large permanent magnets, which constitute the external magnetic field, on the trajectory of implants (small permanent magnets) in the magnetic stereotaxic system. In order to achieve this, we designed a new experimental protocol [9, 10].

MATERIAL AND METHODS

Experimental design: Use two cylindrical large permanent magnets [11–13] to form an external magnetic field, small permanent magnets as implants, and at the same time construct a cylindrical shape with a diameter of 0.1 [m] as a boundary, according to the previous experimental results, the first large permanent magnet is located on the boundary side, the second large permanent magnet is located on the adjacent other side, when the first large permanent magnet runs 0.05 [m], the second large permanent magnet is started, and the two large permanent magnets have the same speed. We set three different sets of large permanent magnet moving speeds, compare the moving distance and angle of small permanent magnets at three speeds, and draw conclusions.

First of all, we carried out computer simulation experiments in COMSOL 6.0 software [14, 15].

Computer simulation experiments

Experimental Objective: To explore the influence of the running speed of large permanent magnets on the motion trajectory of small permanent magnets.

Experimental design: Establish a three-dimensional spatial coordinate system, set small permanent magnets in the center position, set boundary conditions, and set large permanent magnets on the +X and +Y axes respectively. Three sets of experiments were carried out, each of which only changed the running speed of large permanent magnets, and the changes

of the movement trajectories of small and medium-sized permanent magnets in the three groups of experiments were observed and compared.

Parameter settings:

Large permanent magnet radius: R_ion = 50 [mm] = 0.05 [m];

Large permanent magnet height: H_ion =10 [mm] = 0.01 [m];

Small permanent magnet radius: r_NFB =0.5 [mm] = 0.0005 [m];

Small permanent magnet height: h_NFB = 2 [mm] = 0.002 [m];

The distance that a small permanent magnet travels along a straight trajectory: 0[m]＜ds ＜0.1 [m].

The angle between the small permanent magnet and the +X axis after moving along the arc trajectory: 0°<n<90°.

Distance from a large permanent magnet on the +X-axis to the center of three-dimensional space: 0.11 [m]＜dis_ion＜ 0.41 [m], That is, the range of movement of large permanent magnets in the X-axis is 0.11–0.41 [m];

Distance from a large permanent magnet on the +Y-axis to the center of three-dimensional space: 0.11 [m]＜dis_ion1＜0.41 [m], that is, the range of movement of large permanent magnets in the Y-axis is 0.11–0.41 [m];

Diameter of cylindrical container: d_con = 200 [mm] = 0.2 [m];

Cylindrical container height: h_con = 500 [mm] = 0.5 [m];

Before the simulation experiment, we actually measured the existing rail system and used the code “delayMicroseconds” to control the speed of the slide rail, and the results were as follows:

Slide rail system running distance: S = 0.3 [m];

DelayMicroseconds (1200), the running time of the slide rail is 57.3 [s], and the speed of the slide rail is 0.0052 [m/s];

DelayMicroseconds (800), the running time of the slide rail is 38.16 [s], and the speed of the slide rail is 0.0079 [m/s];

DelayMicroseconds (400), the running time of the slide rail is 18.7 [s], and the speed of the slide rail is 0.016 [m/s];

Simulation experiment material property settings:

Conductivity $\sigma = 1/1.4$ [S/m];

Relative permittivity $\varepsilon_r = 1$ [1];

Recovery permeability $\mu_{rec} = 1.02$;

Residual flux density norm $B_r = 1.3$ [T];

The above parameters can be changed according to the actual material data. Based on the above parameters, the geometry is established in COMSOL, as shown in Fig. 1.

In this simulation experiment, we choose a permanent magnet as the external magnetic field, so we need to select “mfnc” (magnetic field, no current) in the software, and select the magnetization model — residual flux density in constitutive relations B-H, and the required equation is as follows:

$$B = \mu_0 \mu_{rec} H + B_r \tag{1}$$

$$B_r = \|B_r\| \frac{\mathbf{e}}{\|\mathbf{e}\|} \tag{2}$$

Where H is the magnetic field strength, B is the magnetic flux density, μ_0 is the vacuum permeability, μ_{rec} is recoil permeability, B_r is residual flux density, $\left\|B_r\right\|$ is residual flux density norm, e is residual flux direction.

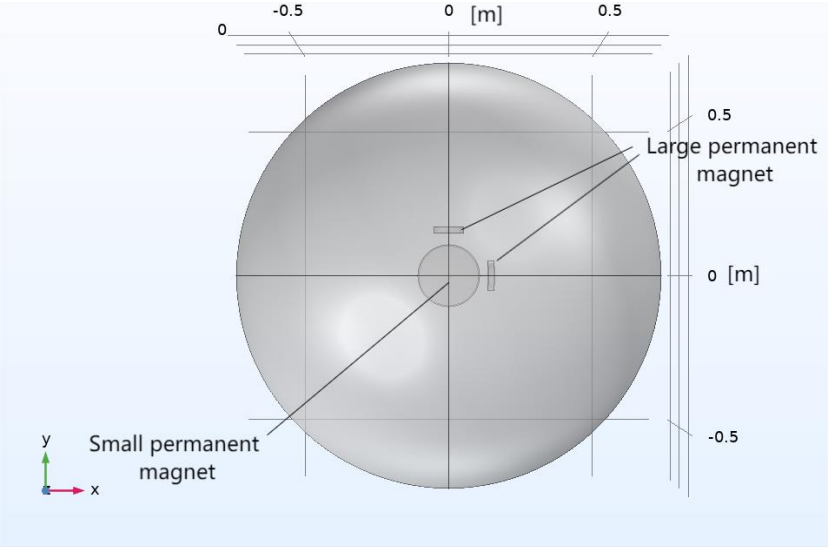

Fig 1. Geometric models based on parameters in COMSOL software.

The first set of experiments

We set up large permanent magnets to move at a slower speed, i.e. 0.0052 [m/s], after the first large permanent magnet moves 0.05 [m], the second large permanent magnet begins to approach the center position, when the first large permanent magnet is 0.18 [m] from the center position, its magnetic field touches the small permanent magnet, the small permanent magnet is affected by its magnetic field, and begins to move to the first large permanent magnet along a straight trajectory, until the first large permanent magnet reaches the maximum moving distance, that is, dis_ion = 0.11 [m], and then the first large permanent magnet begins to gradually move away from the center position, The second large permanent magnet is still approaching the center, which is dis_ion<dis_ion1 in the process, as shown in Fig. 2. The coloured bands on the right indicate the strength of the magnetic field in [T] represented by the different coloured areas in the picture.

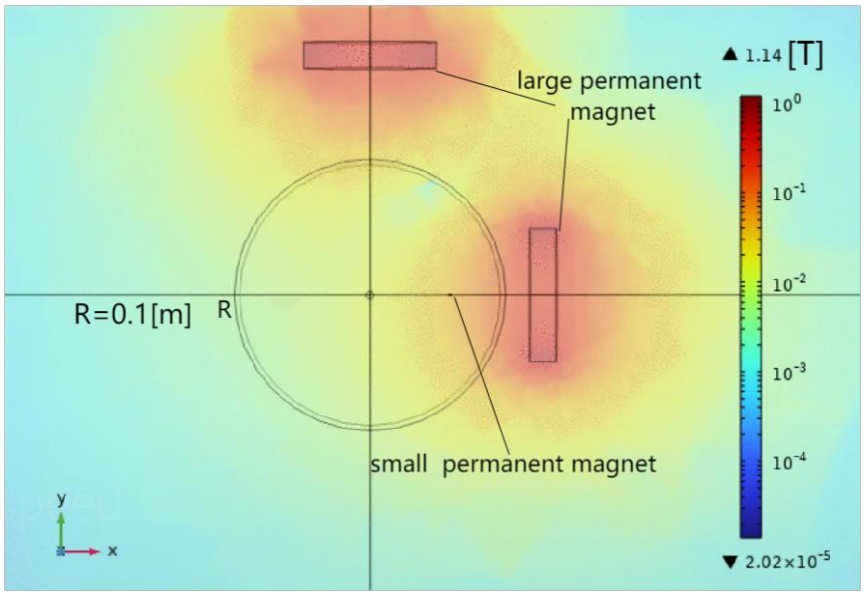

Fig 2. The small permanent magnet begins to move along a straight trajectory towards the first large permanent magnet. The boundary radius is R. The maximum radius of motion of a small permanent magnet is R.

When the first large permanent magnet gradually moves away from the center position, 0.13 [m] from the center position, and the second large permanent magnet gradually approaches the center position, 0.14 [m] from the center position, that is, dis_ion = 0.13 [m], dis_ion = =0.14 [m], at this time the small permanent magnet stops moving, 0.09 [m] from the center position, that is, the small permanent magnet moves 0.09 [m] along a straight trajectory, that is, ds = 0.09 [m], as shown in Fig. 3, a.

After that, the first large permanent magnet continues away from the center position, the second large permanent magnet is close to the center position until it is 0.11 [m] from the center position, that is, dis_ion1 = 0.11 [m], and the second large permanent magnet begins to gradually move away from the center position. In the process, dis_ion>dis_ion1, the small permanent magnet begins to move along an arc trajectory towards the second large permanent magnet. When the second large permanent magnet moves 0.2 [m] from the center position, and the first large permanent magnet moves 0.25 [m] from the center position, the small permanent magnet is free from the influence of the external magnetic field and stops moving, at this time the angle between the small permanent magnet and the +X axis is n=30°, that is, the small permanent magnet moves $^1/_{12}$ of a circle along the arc trajectory, as shown in Fig. 3, b.

The second set of experiments

We set large permanent magnets to run at moderate speeds, i.e. 0.0079[m/s], other conditions remain unchanged. When dis_ion<dis_ion1, the small permanent magnet moves along a straight trajectory towards the first large permanent magnet. When dis_ion = 0.13 [m], dis_ion1 = 0.14 [m], we can clearly see that the small permanent magnet has not reached the position of the previous set of experiments, and the small permanent magnet is ds = 0.0675 [m] from the center, as shown in Fig. 3, c.

After that, the first large permanent magnet continues away from the center, the second large permanent magnet first approaches and then moves away from the center, and at this stage, the dis_ion>dis_ion1, small permanent magnet begins to move along an arc trajectory towards the second large permanent magnet. When dis_ion1 = 0.2 [m], dis_ion = 0.25 [m], the small permanent magnet breaks away from its magnetic field and stops moving. At this time, we can clearly observe that the angle between the small permanent magnet and the +X axis exceeds the data of the previous set of experiments, and the angle between the small permanent magnet and the +X axis is n=45°, that is, the small permanent magnet moves $^1/_8$ of a circle along the arc trajectory, as shown in Fig. 3, d.

The third set of experiments

We set large permanent magnets to run at a relatively fast speed, i.e. 0.016 [m/s], other conditions remain unchanged. When dis_ion<dis_ion1, the small permanent magnet moves along a straight trajectory towards the first large permanent magnet. When dis_ion=0.13[m], dis_ion1 = 0.14 [m], we can clearly see that the small permanent magnet has not reached the position of the previous two set of experiments, and the small permanent magnet is ds = =0.045 [m] from the center, as shown in Fig. 3, e.

After that, the first large permanent magnet continues to move away from the center, the second large permanent magnet first approaches and then moves away from the center, and at this stage, the small permanent magnet dis_ion>dis_ion1 begins to move along an arc trajectory towards the second large permanent magnet. When dis_ion = 0.25 [m], dis_ion1 = 0.2 [m], the small permanent magnet breaks away from its magnetic field and stops moving. At this point, we can clearly see that the angle of movement of the small permanent magnet

along the arc trajectory exceeds the angle of the previous two sets of experiments, and the angle between the small permanent magnet and the +X axis is n = 60°, that is, the small permanent magnet moves $^1/_6$ of a circle along the arc trajectory, as shown in Fig. 3, f.

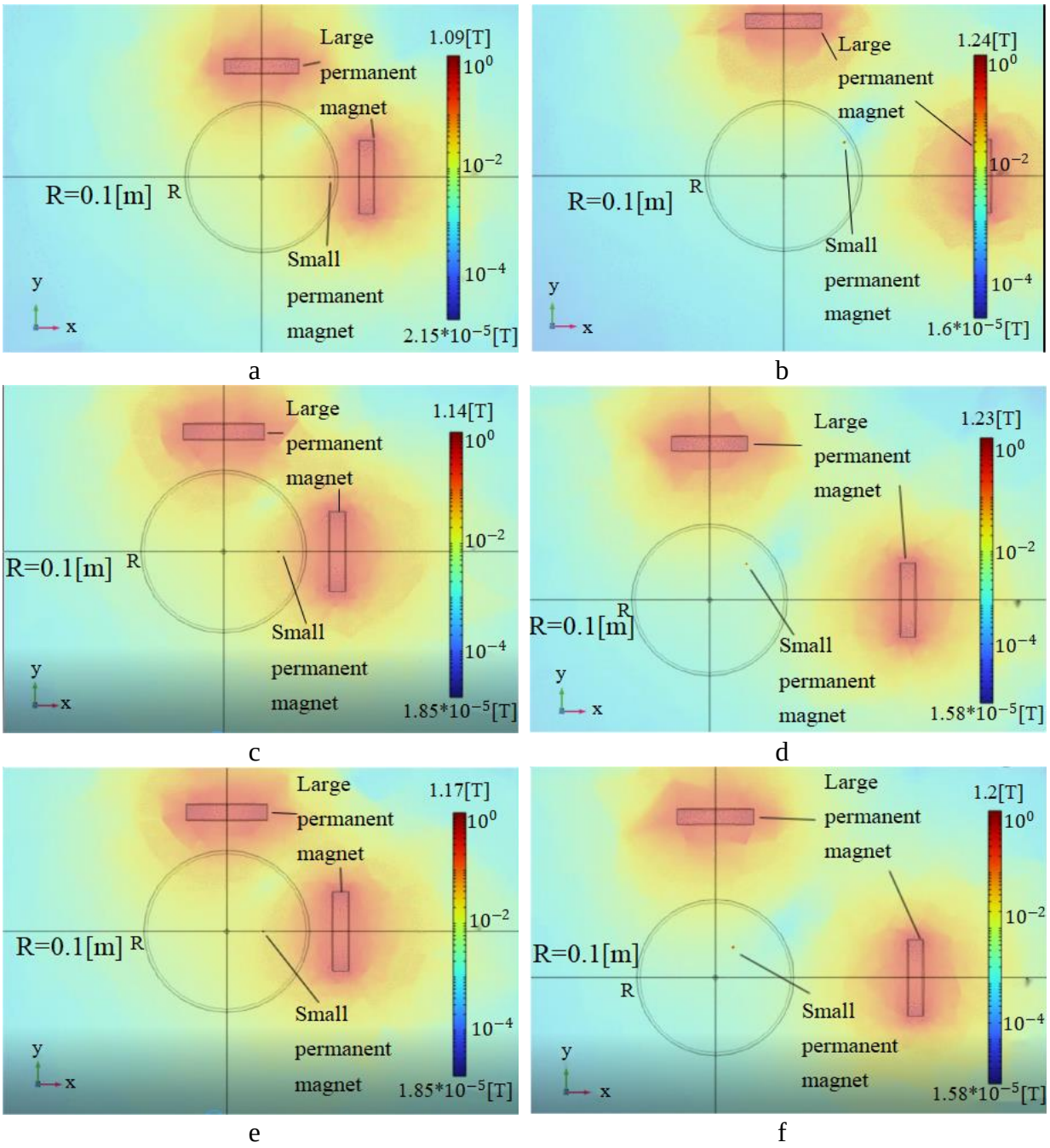

Fig 3. a, b are the first set of simulation experiments; c, d are the second set of simulation experiments; e, f are the third set of simulation experiments. The boundary radius is R. The maximum radius of motion of a small permanent magnet is R. Fig 3, a. dis_ion = 0.13 [m], dis_ion1 = 0.14 [m], the small permanent magnet stopped moving, and ds = 0.09 [m]. Fig 3, b. dis_ion = 0.25 [m], dis_ion1 = 0.2 [m], the small permanent magnet stops moving, and the angle to the +X axis is n = 30°. Fig 3, c. dis_ion = 0.13 [m], dis_ion1 = 0.14 [m], the small permanent magnet stopped moving, and ds = 0.0675 [m]. Fig 3, d. When the movement stops, the angle between the small permanent magnet and the +X axis is n = 45°. Fig 3, e. dis_ion = 0.13 [m], dis_ion1 = 0.14 [m], the small permanent magnet stopped moving, and ds = 0.045 [m]. Fig 3, f. dis_ion = 0.25 [m], dis_ion1 = 0.20 [m], n = 60°, the small permanent magnet stops moving.

In order to see the results of the computer simulation experiments more intuitively, we made tables of the moving speed of the large permanent magnet, the distance moved by the small permanent magnet along the straight line trajectory, and the angle between the final resting position of the small permanent magnet and the +X axis according to the above experimental data as shown in the table below.

Table 1. Effect of large permanent magnet movement speed on small permanent magnet movement trajectory.

V [m/s]	Ds [m]	N [°]
0.0052	0.09	30
0.0079	0.0675	45
0.016	0.045	60

Where V is the operating speed of the large permanent magnet; ds is the distance moved by the small permanent magnet along the straight line trajectory; n is the angle between the location of the small permanent magnet after moving along the arc trajectory and the +X axis.

Practical experiments

Experimental Objective: The results of computer simulation experiments were verified to determine the influence of the movement speed of large permanent magnets on the movement trajectory of small permanent magnets.

Experimental design: The working environment of the implant is simulated by a slightly solidified jelly-like gelatin solution, and a small permanent magnet connected by a catheter is placed in the center of the container containing the gelatin solution, and the external magnetic field consists of two slide rail systems equipped with large permanent magnets, which are controlled by the Arduino UNO [16, 17]. Three sets of experiments were carried out, and the slide rail system was based on 0.0052 [m/s], 0.0079 [m/s], 0.016 [m/s] three speed movements, observe the running trajectories of small permanent magnets in each group of experiments and compare them.

Equipment and materials required for the experiment: Two Arduino UNO microcontrollers, two large permanent magnets, one small permanent magnet, 5% gelatin solution, two sets of ball screw slides with 57×56 stepper motors, stepper motor controller, external power supply, cylindrical container with a diameter of 0.2 [m], conduit, several wires.

Experimental equipment assembly: The ball screw slide rail equipped with a large permanent magnet is controlled by the Arduino controller, and the slide rail system is driven by a 57×56 stepper motor with a running distance of 0.3[m]. The stepper motor has four wires that connect it to the four interfaces of the stepper motor controller: The red wire is connected to A+; Green wire is connected to A-; Yellow wire connected to B+; Blue wire connection to B-. Then connect the stepper motor controller with the Arduino controller: Connect PUL-, DIR-, EN- together, and connect to the Arduino's GND, PUL+ is connected to the 9-pin of the Arduino and controls stepper motor operation, DIR+ is connected to the Arduino's 8-pin and controls the stepper motor's direction of rotation, EN+ is connected to the Arduino's GND or can also be left unconnected. Then connect the V+ of the external power supply to the V+ of the stepper motor controller, connect the V- of the external power supply to the GND of the stepper motor controller, and finally connect the computer and the arduino controller through the data line, so that a set of slide rail system is completed. The two sets of assembled slide rail systems were placed on the adjacent sides of the container, the configured 5% gelatin solution was poured into the container, and it stood for two hours, and after the

gelatin solution in the container was jelly-like, the small permanent magnet was connected to the catheter and placed in the center of the container, at this point, the experimental equipment is assembled. The practical experimental equipment is shown in Fig. 4.

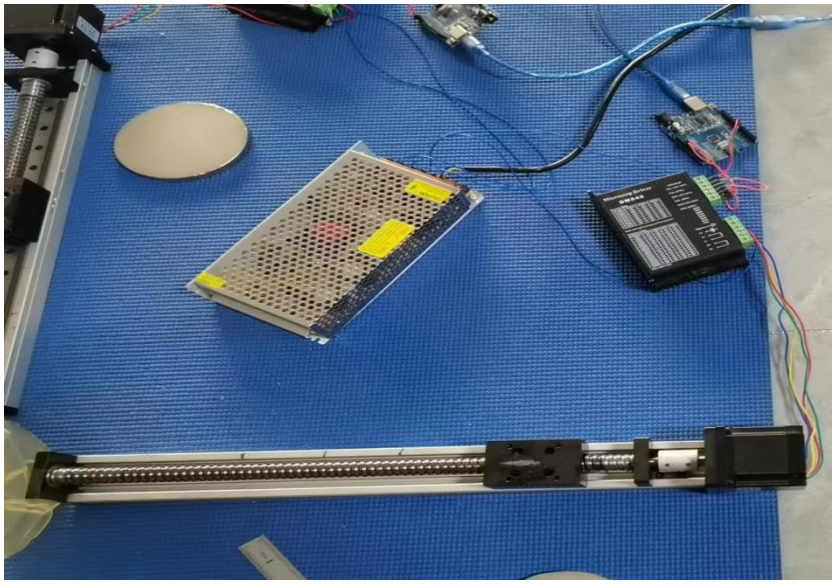

Fig 4. Slide rail system controlled by an Arduino controller.

The first set of experiments

First we set the slide rail system to run at a slower speed, that is, the large permanent magnet runs at a 0.0052 [m/s] movement. Start the first slide rail system after the power is applied, and start the second slide rail system after it runs 0.05 [m]. When the distance from the first large permanent magnet to the container boundary is less than the distance from the second large permanent magnet to the container boundary, that is, dis_ion<dis_ion1, as shown in Fig. 5, a, we can clearly see that the small permanent magnet has moved a long distance along a straight trajectory and is very close to the container boundary.

After that, the first large permanent magnet continues to move away, and the second large permanent magnet first approaches and then moves away, that is, dis_ion>dis_ion1, the small permanent magnet moves along the arc trajectory towards the second large permanent magnet. When they were far enough away, the small permanent magnets stopped moving, and we could clearly see that the small permanent magnets had only moved a short distance along the arc trajectory, as shown in Fig. 5, b.

The second set of experiments

We set the slide rail system to run at a moderate speed with a movement speed of 0.0079 [m/s]。 After the first large permanent magnet runs 0.05 [m], the second large permanent magnet begins to move. In the dis_ion<dis_ion1 phase, it is clear that the small permanent magnets move along a straight trajectory, but the distance is less than the distance that the small permanent magnets moved along the straight trajectory in the first set of experiments. As shown in Fig. 5, c.

After that, in the dis_ion>dis_ion1 phase, the small permanent magnet begins to move along an arc trajectory towards the second large permanent magnet. When they were far enough away from the small permanent magnets to stop moving, we were able to observe that the small permanent magnets moved a distance along the arc trajectory, significantly more than the distance the small permanent magnets in the first set of experiments moved along the arc trajectory. As shown in Fig. 5, d.

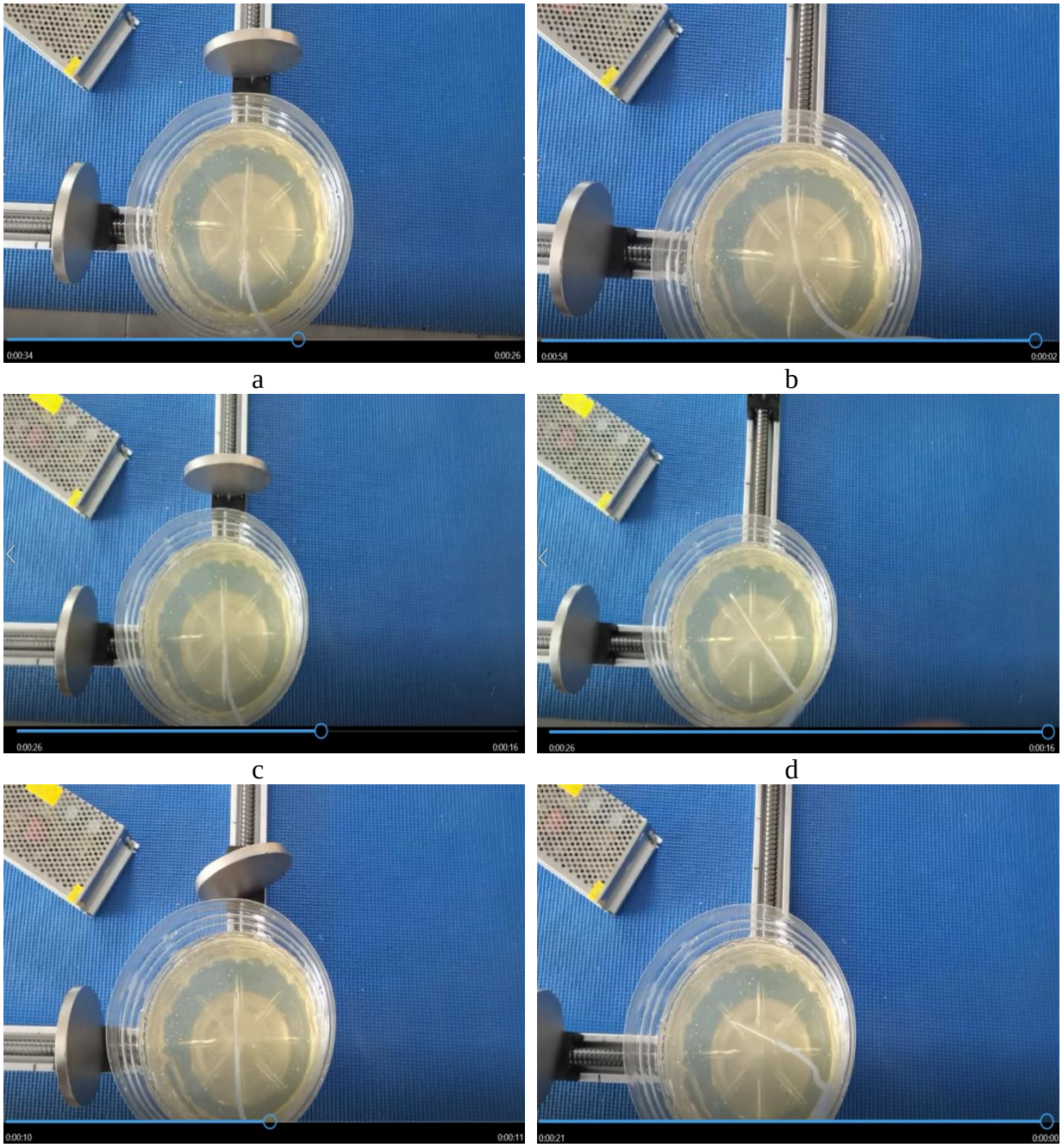

Fig 5. a, b are the first set of experiments; c,d are the second set of experiments; e, f are the third set of experiments.

Fig a. When the slide system runs at a slower speed, small permanent magnets move along a straight trajectory and approach the container boundary.

Fig b. At dis_ion>dis_ion1, small permanent magnets can only move a short distance along an arc trajectory.

Fig c. When the slide rail system moves at moderate speeds, the small permanent magnets move less distance along a straight trajectory than the results of the first set of experiments.

Fig d. The small permanent magnet moved some distance along the arc trajectory.

Fig e. Small permanent magnets move shorter distances in a straight line than in the first two sets of experiments.

Fig f. The small permanent magnet traveled a long distance along the arc trajectory.

The third set of experiments

We set the slide rail system to run at a faster speed, i.e. move at a speed of 0.016 [m/s]. During the dis_ion<dis_ion1 phase, as shown in Fig. 5, e we were able to see the small permanent magnets moving along a straight trajectory, but the distance traveled was the shortest of the three sets of experiments.

After that, in the dis_ion>dis_ion1 phase, the small permanent magnet begins to move along the arc trajectory towards the second large permanent magnet. When they moved far enough from the small permanent magnets to stop moving, we could clearly see that the small permanent magnets moved significantly farther along the arc trajectory than the previous two sets of experiments. As shown in Fig. 5, f.

In addition, it should be noted that because the gelatin solution will gradually solidify with time, and the change of external temperature will also have a certain impact on the gelatin solution, which leads to certain errors between the results of the actual experiment and the results of the computer simulation experiment, so it is necessary to try to ensure that the three sets of experiments are completed within a certain time.

RESULTS AND DISCUSSION

Simulation experiment conclusion

Through computer simulation experiments we found:

1. When large permanent magnets move slowly, i.e. 0.0052 [m/s], in the dis_ion<dis_ion1 stage, the small permanent magnet traveled the longest distance along the linear trajectory, ds= = 0.09 [m]. In the dis_ion>dis_ion1 stage, the angle between the small permanent magnet and the +X axis is the smallest after moving along the arc trajectory, n = 30°.

2. When large permanent magnet moves at a moderate speed, i.e. 0.0079 [m/s], in the dis_ion<dis_ion1 stage, the small permanent magnet moved along a straight trajectory in the middle position of the three sets of experiments, ds = 0.0675 [m]. In the dis_ion>dis_ion1 stage, the angle between the small permanent magnet and the +X axis after moving along the arc trajectory is also in the middle position of the three sets of experiments, n = 45°.

3. When large permanent magnets move at a relatively fast speed, i.e. 0.016 [m/s], in the dis_ion<dis_ion1 stage, the small permanent magnet travels the shortest distance along the linear trajectory, ds = 0.045 [m]. In the dis_ion>dis_ion1 stage, the angle between the small permanent magnet and the +X axis after moving along the arc trajectory is the largest, n = 60°.

Practical experimental conclusions

The results of this practical experiment show that the results of computer simulation experiments are real and reliable. By comparing the three sets of actual experiments, we found that:

1. The slide rail system starts with 0.0052 [m/s] speed operation, in the dis_ion<dis_ion1 stage, small permanent magnets move along a straight trajectory, and their travel distance is the longest in the three sets of experiments; In the dis_ion>dis_ion1 stage, the small permanent magnet moves along the arc trajectory, and the angle between the position of the small permanent magnet and the linear trajectory is the smallest in the three sets of experiments, that is, the distance of the small permanent magnet moving along the arc trajectory is the shortest.

2. The slide rail system starts with 0.0079 [m/s] speed operation, in the dis_ion<dis_ion1 phase, small permanent magnets move along a straight trajectory, and their moving distance is in the middle position in the three sets of experiments; In the dis_ion>dis_ion1 stage, the small permanent magnet moves along the arc trajectory, and the angle between the position of

the small permanent magnet and the linear trajectory is also in the middle position in the three sets of experiments, that is, the distance of the small permanent magnet moving along the arc trajectory is in the middle position of the three sets of experimental results.

3. The slide rail system starts with 0.016 [m/s] speed operation, in the dis_ion<dis_ion1 stage, small permanent magnets move along a straight trajectory, and their travel distance is the shortest of the three sets of experiments; In the dis_ion>dis_ion1 stage, the small permanent magnet moved along the arc trajectory, and the angle between the position of the small permanent magnet and the linear trajectory was the largest in the three sets of experiments, that is, the distance traveled by the small permanent magnet along the arc trajectory was the longest in the three sets of experimental results.

Through computer simulation experiments and practical experiments, we get the following conclusions: the faster the moving speed of the large permanent magnet that constitutes the external magnetic field in the magnetic stereotaxic system, the shorter the distance that the small permanent magnet as an implant moves along the straight line trajectory, and the longer the distance that it moves along the arc trajectory; the slower the moving speed of the large permanent magnet, the longer the distance that the small permanent magnet moves along the straight line trajectory, and the shorter the distance that it moves along the arc trajectory.

CONCLUSION

In this research, we have determined the relationship between the running speed of the large permanent magnet that constitutes the external magnetic field and the implant's moving trajectory by combining computer simulation experiments with practical experiments, i.e., the faster the large permanent magnet moves, the shorter the implant's moving distance is along a straight line trajectory, and the longer the moving distance is along a curved line trajectory. This means that we can control the distance and steering angle of the implant more accurately, which makes the study of the magnetic stereotaxic system further, and lays a theoretical foundation and provides a large amount of experimental data for the implant to be able to reach the diseased site located in the deep structure of the brain tissue along complex pathways in neurosurgical interventions with the participation of the magnetic stereotaxic system.

CONFLICT OF INTEREST

The authors declare that there is no conflict of interest.

Authors' ORCID ID

Hankun Jiao https://orcid.org/0000-0003-0992-5344
Oleg Avrunin https://orcid.org/0000-0002-6312-687X

REFERENCES

1. Grady SM, Howard III MA, Broaddus WC, Molloy JA, Ritter RC, Quate EG, Gillies GT. Magnetic stereotaxis: a technique to deliver stereotactic hyperthermia. Neurosurgery. 1990 Dec 1;27(6):1010–6. https://doi.org/10.1097/00006123-199012000-00026
2. Nelson BJ, Gervasoni S, Chiu PW, Zhang L, Zemmar A. Magnetically actuated medical robots: An in vivo perspective. Proceedings of the IEEE. 2022 Apr 28;110(7):1028–37. https://doi.org/10.1109/JPROC.2022.3165713
3. Grady MS, Howard MA, Dacey RG, Blume W, Lawson M, Werp P, Ritter RC. Experimental study of the magnetic stereotaxis system for catheter manipulation within the brain. Journal of neurosurgery. 2000 Aug 1;93(2):282–8. https://doi.org/10.3171/jns.2000.93.2.0282
4. Avrunin O, Tymkovych M, Semenets V, Piatykop V. Computed tomography dataset analysis for stereotaxic neurosurgery navigation. In: 2019 IEEE 8th International Conference on Advanced Optoelectronics and Lasers (CAOL); 2019 Sep 6; IEEE. p. 606–9).. https://doi.org/10.1109/CAOL46282.2019.9019459

5. Avrunin OG, Alkhorayef M, Saied HF, Tymkovych MY. The surgical navigation system with optical position determination technology and sources of errors. Journal of Medical Imaging and Health Informatics. 2015 Aug 1;5(4):689–96. https://doi.org/10.1166/jmihi.2015.1444
6. Avrunin OG, Tymkovych MY, Moskovko SP, Romanyuk SO, Kotyra A, Smailova S. Using a priori data for segmentation anatomical structures of the brain. Przegląd Elektrotechniczny. 2017 May 1;3:102–5. https://doi.org/10.15199/48.2017.05.20
7. Chen Y, Godage I, Su H, Song A, Yu H. Stereotactic systems for MRI-guided neurosurgeries: a state-of-the-art review. Annals of biomedical engineering. 2019 Feb 15;47:335–53. https://doi.org/10.1007/s10439-018-02158-0
8. Withers PJ, Bouman C, Carmignato S, Cnudde V, Grimaldi D, Hagen CK, Maire E, Manley M, Du Plessis A, Stock SR. X-ray computed tomography. Nature Reviews Methods Primers. 2021 Feb 25;1(1):18. https://doi.org/10.1038/s43586-021-00015-4
9. Hankun J, Avrunin O. Explore the feasibility study of magnetic stereotaxic system. Optoelectronic Information-Power Technologies. 2023 Sep;45(1):86–96. https://doi.org/10.31649/1681-7893-2023-45-1-86-96
10. Hankun J, Avrunin O. Possibilities of Field Formation by Permanent Magnets in Magnetic Stereotactic Systems. In: 2022 IEEE 3rd KhPI Week on Advanced Technology (KhPIWeek); 2022 Oct 3; IEEE. p. 1–4. https://doi.org/10.1109/KhPIWeek57572.2022.9916450
11. O'Reilly T, Teeuwisse WM, de Gans D, Koolstra K, Webb AG. In vivo 3D brain and extremity MRI at 50 mT using a permanent magnet Halbach array. Magnetic resonance in medicine. 2021 Jan;85(1):495–505. https://doi.org/10.1002/mrm.28396
12. Brown D, Ma BM, Chen Z. Developments in the processing and properties of NdFeB-type permanent magnets. Journal of magnetism and magnetic materials. 2002 Aug 1;248(3):432–40. https://doi.org/10.1002/chin.200311225
13. Calin MD, Helerea E. Temperature influence on magnetic characteristics of NdFeB permanent magnets. In: 2011 7th international symposium on advanced topics in electrical engineering (ATEE); 2011 May 12; IEEE. p. 1–6.
14. Multiphysics CO. Introduction to COMSOL multiphysics®. COMSOL Multiphysics, Burlington, MA, accessed Feb. 1998 Feb;9(2018):32.
15. Pepper DW, Heinrich JC. The finite element method: basic concepts and applications with MATLAB, MAPLE, and COMSOL. CRC press; 2017 Apr 11. http://doi.org/10.1201/9781315395104
16. Badamasi YA. The working principle of an Arduino. In: 2014 11th international conference on electronics, computer and computation (ICECCO); 2014 Sep 29; IEEE. p. 1–4. https://doi.org/10.1109/ICECCO.2014.6997578
17. Banzi M, Shiloh M. Getting started with Arduino. Maker Media, Inc.; 2022 Feb 15.
18. Sokol Y, Avrunin O, Kolisnyk K, Zamiatin P. Using medical imaging in disaster medicine. In: 2020 IEEE 4th International Conference on Intelligent Energy and Power Systems (IEPS); 2020 Sep 7; IEEE. p. 287–90). https://doi.org/10.1109/IEPS51250.2020.9263175
19. Avrunin O, Kolisnyk K, Nosova Y, Tomashevskyi R, Shushliapina N. Improving the methods for visualization of middle ear pathologies based on telemedicine services in remote treatment. In: 2020 IEEE KhPI Week on Advanced Technology (KhPIWeek); 2020 Oct 5; IEEE. p. 347–50. https://doi.org/10.1109/KhPIWeek51551.2020.9250090

ВИЗНАЧЕННЯ ВЗАЄМОЗВ'ЯЗКУ МІЖ ШВИДКІСТЮ РУХУ ВЕЛИКИХ ПОСТІЙНИХ МАГНІТІВ І ТРАЄКТОРІЄЮ РУХУ ІМПЛАНТАТІВ У МАГНІТНИХ СТЕРЕОТАКСИЧНИХ СИСТЕМАХ

Ц. Ханькунь, О. Г. Аврунін
Харківський національний університет радіоелектроніки, проспект Науки, 14, Харків, 61166, Україна
e-mail: 1350829683@qq.com, oleh.avrunin@nure.ua
Надійшла до редакції 9 листопада 2023 р. Переглянута 17 січня 2024 р.
Прийнята до друку 20 березня 2024 р.

Актуальність. Магнітна стереотаксична система — це новий вид нейрохірургічного втручання, який знаходиться на стадії експерименту. Цей метод дозволяє безконтактно керувати імплантатом за допомогою зовнішнього магнітного поля, дозволяючи йому рухатися по довільній траєкторії до вогнища ураження, розташованого в глибоких структурах мозкової тканини, щоб доставити гіпертермію до місця ураження або доставити ліки через катетер. У попередніх дослідженнях ми виявили, що рух імплантату по дуговій траєкторії цілком можливий, тому нам необхідно

визначити зв'язок між швидкістю руху великого постійного магніту, що становить зовнішнє магнітне поле, і траєкторією руху імплантату, щоб більш точно керувати рухом імплантату.
Мета — дослідити вплив швидкості руху великих постійних магнітів, що складають зовнішнє магнітне поле, на траєкторію руху імплантатів (малих постійних магнітів).
Матеріали і методи. Спочатку було проведено три серії комп'ютерних імітаційних експериментів, в кожній групі експериментів змінювалася тільки швидкість роботи великих постійних магнітів, а також спостерігалися і порівнювалися зміни траєкторій малих і середніх постійних магнітів в трьох серіях експериментів. Після цього були проведені практичні експерименти для перевірки результатів комп'ютерного моделювання експериментів за допомогою рейкової системи, керованої мікроконтролером Arduino.
Результати. За допомогою імітаційних експериментів визначено зв'язок між швидкістю переміщення великого постійного магніту та траєкторією руху малого постійного магніту, а також розраховано зміни напруженості навколишнього магнітного поля під час руху імплантату. Після цього це було перевірено практичними експериментами. Чим швидше рухається великий постійний магніт, тим меншу відстань малий постійний магніт проходить по лінійній траєкторії, а більшу — по дуговій; чим повільніше рухається великий постійний магніт, тим більшу відстань малий постійний магніт проходить по прямій траєкторії, а меншу — по дуговій траєкторії.
Висновки. У цьому дослідженні ми визначили взаємозв'язок між швидкістю руху великого постійного магніту, що становить зовнішнє магнітне поле, і траєкторією руху імплантату, поєднавши комп'ютерні симуляційні експерименти з практичними експериментами, тобто чим швидше рухається великий постійний магніт, тим коротша відстань переміщення імплантату по прямій траєкторії, і тим довша відстань переміщення по криволінійній траєкторії. Це означає, що ми можемо більш точно контролювати відстань і кут повороту імплантату, що сприяє подальшому вивчення магнітної стереотаксичної системи, а також закладає теоретичний фундамент і забезпечує велику кількість експериментальних даних для того, щоб імплантат міг досягти хворої ділянки, розташованої в глибокій структурі тканини мозку по складних шляхах при нейрохірургічних втручаннях за участю магнітної стереотаксичної системи.
КЛЮЧОВІ СЛОВА: здоров'я людини; магнітне поле; програмне забезпечення COMSOL; постійні магніти; силовий аналіз; Arduino; мікроконтролери.